protein denaturation resulting from binding of the RC complex to the Ag electrode surface during SERRS experiments should affect the structure of the heme group and hence its resonance Raman spectrum. Smulevich and Spiro claim that any major distortion of the heme active site gives rise to new resonance Raman spectral peaks at 1490 and 1570 cm^{-1} due to the formation of electrode-surface-bound hemin oxo dimers.[7] Also, it is important to note here that the results of Hildebrandt and Stockburger[37,38] have shown that a temperature-dependent, reversible spin-state change occurs in Cyt *c* when adsorbed on colloidal silver. However, even these reversible perturbations of the protein structure can be avoided, as we have succeeded in developing a Ag sol preparation that does not produce these spin-state changes.[39] Thus, in the results obtained here, no new peaks are observed at the positions indicative of oxo dimer formation or of spin-state changes, and we conclude that the PSII RC complex is also stable on the Ag electrode surface.

Since no evidence for structural protein damage is observed when bacterial or PSII RC complexes are adsorbed on Ag electrode surfaces,[40] SERRS spectroscopy appears to be a reliable technique for studying purified complex chromoproteins. Furthermore, the fact that the potential applied to SERRS-active electrodes can be varied makes this technique very promising for detecting intermediate redox species in redox-active chromoproteins, such as photochemically active RCs.

Acknowledgment. We thank Stephen P. Toon for preparing the PSII reaction centers and Jae-Ho Kim for assembling some of the data. M.S. thanks the Onyx Chemical Co. of Jersey City, NJ for its generous gift of LDAO used in this study. This work was supported by the Divisions of Chemical Sciences (M.S. and T.M.C.) and Energy Biosciences (M.S.), Office of Basic Energy Sciences, U.S. Department of Energy, and Consejo Superior de Investigaciones Cientificas, Spain (R.P.). Ames Laboratory is operated for the U.S. Department of Energy by Iowa State University under Contract No. W-7405-Eng-82. SERI is a division of the Midwest Research Institute and operated for the U.S. Department of Energy under Contract No. DE-AC02-83CH-10093.

Registry No. Pheo *a*, 603-17-8; Cyt *b*-559, 9044-61-5; Chl *a*, 479-61-8; Spx, 34255-08-8; Ag, 7440-22-4; β-carotene, 7235-40-7.

(37) Hildebrandt, P.; Stockburger, M. *J. Phys. Chem.* **1986**, *90*, 6017-6024.
(38) Hildebrandt, P.; Stockburger, M. *Biochemistry* **1989**, *28*, 6710-6721.
(39) Rospendowski, B. N.; Schlegel, V. L.; Holt, R. E.; Cotton, T. M. *Charge and Field Effects in Biosytems—2*; Allen, M. J., Cleary, S. F., Hawkridge, F. M., Eds.; Plenum Publishing: 1989; pp 43-58.
(40) It is likely that reaction centers adsorb to the Ag electrode in several different orientations. Since there is such an extreme distance effect in SERRS, only those orientations that bring either the spirilloxanthin or the Cyt *b*-559 in near proximity to the Ag electrode will contribute to our spectral observations.

Resonance Raman Characterization of Nitric Oxide Adducts of Cytochrome P450cam: The Effect of Substrate Structure on the Iron–Ligand Vibrations

Songzhou Hu and James R. Kincaid*

Contribution from the Chemistry Department, Marquette University, Milwaukee, Wisconsin 53233. *Received April 9, 1990*

Abstract: Resonance Raman spectra of the nitric oxide adducts of ferric cytochrome P450cam are acquired with Soret excitation. The frequencies of the heme skeletal vibrations are found 3–10 cm^{-1} lower than those of horseradish peroxidase and myoglobin. The axial vibrations are located and assigned by isotopic substitution. The stretching, ν(Fe–NO), and bending, δ(Fe–N–O), modes are detected at 522 and 546 cm^{-1}, respectively, for the title adduct in the presence of camphor. They shift to 520 and 533 cm^{-1} upon substitution by $^{15}N^{16}O$. The strong line at 522 cm^{-1} shifts to 528 cm^{-1} when the substrate is removed from the active site, whereas it appears at 524 cm^{-1} upon the addition of norcamphor. The isotopic sensitivity of these bands confirms their assignment as ν(Fe–NO). It is observed that only the larger substrates (camphor and adamantanone) give rise to the enhancement of the bending mode δ(Fe–N–O). As the substrate size increases, a band of medium intensity, which is tentatively assigned as ν(Fe–S), increases from 349 cm^{-1} (substrate free) to 359 cm^{-1} (adamantanone). On the basis of the consideration of both the electronic factors and the kinematic effect of distortion of the Fe–NO unit, it is suggested that the Fe–NO linkage adopts a linear structure in the absence of substrate but becomes slightly bent in the presence of substrates.

Introduction

The generic name, cytochrome P450, was given to a class of heme-containing enzymes that give rise to the electronic absorption maxima around 450 nm upon the formation of ferrous carbonyl complexes.[1] These b-type hemoproteins play a very important role in a wide variety of hydroxylation reactions, the oxidizing center being generated by two-electron reduction and cleavage of dioxygen.[2] Among the various cytochromes P450 that have been isolated and purified, that known as cytochrome P450cam, derived from *P. putida*, has been most thoroughly characterized, owing to its relative ease of isolation and aqueous solubility.[3]

(1) (a) Ortiz de Montellano, P. R., Ed. *Cytochrome P450 Structure, Mechanism, and Biochemistry*; Plenum Press: New York, 1986. (b) Schuster, I., Ed. *Cytochrome P450: Biochemistry and Biophysics*; Traylor & Francis, 1989. (c) Sato, R., Omura, T., Eds. *Cytochrome P450*; Academic Press: New York, 1978.
(2) (a) Black, S. D.; Coon, M. J. *Adv. Enzymol. Relat. Areas Mol. Biol.* **1987**, *60*, 35-87. (b) Dawson, J. H. *Science* **1988**, *240*, 433-439. (c) Guengerich, F. P.; McDonald, T. L. *Acc. Chem. Res.* **1984**, *17*, 9-16. (d) Dawson, J. H.; Sono, M. *Chem. Rev.* **1987**, *87*, 1255-1276. (e) Sligar, S. G.; Gelb, M. H.; Heimbrook, D. C. *Xenobiotica* **1984**, *14*, 63-86.
(3) (a) Murray, R. I.; Fisher, M. T.; Debrunner, G.; Sligar, S. G. In *Metalloproteins Part I: Metal Proteins with Redox Roles*; Harrison, P. M., Ed.; Verlag Chemie: Weinheim, 1985; p 157. (b) Dawson, J. H.; Eble, K. S. *Adv. Inorg. Bioinorg. Mech.* **1986**, *4*, 1-64.

0002-7863/91/1513-2843$02.50/0

Recently, the high-resolution crystal structures of cytochrome P450cam in the oxidized state have been reported for both the substrate-free and several substrate-bound forms of the enzyme.[4] They provide a clear rationale for the unusual optical properties that are associated with a specific axial ligand (the mercaptide sulfur of cysteine), the conversion from a low-spin to a high-spin state, and the marked elevation of the redox potential of the heme when camphor is bound to the ferric cytochrome P450cam.

Resonance Raman (RR) spectroscopy is a powerful technique for probing the active site of hemoproteins.[5] The acquisition of RR spectra of model compounds has greatly improved the current understanding of the interactions of the heme group with protein residues around the heme pocket.[6] Detailed RR investigations of the stable reaction states[7] and the oxygenated intermediate[8] of cytochrome P450cam have been reported previously. The RR enhancement of the Fe–S stretching mode at 351 cm^{-1} provides definitive evidence for the presence of an Fe–S linkage in cytochrome P450cam.[9] A detailed study of carbon monoxide adducts was made in order to probe the interaction of substrate with ferrous cytochrome P450cam.[10]

Nitric oxide is able to bind to both ferric and ferrous heme proteins and heme model compounds. These systems are of interest because they are similar in electronic structure and geometry to the physiologically important dioxygen complexes of hemoproteins. Ferrous nitrosyl complexes have been extensively studied by X-ray,[11] ESR,[12] IR,[13] Mössbauer,[14] and RR[15] as well as theoretical calculations[16] and were utilized to study the dynamics and conformational changes of hemoglobin.[15d] On the other hand, ferric nitrosyl adducts, owing to their intrinsic instability toward autoreduction, are not well understood and are rarely used to probe the structure of ferric heme proteins. The diamagnetism prevents the use of ESR and the high quantum yield[17] of ligand photodissociation makes resonance Raman studies quite difficult. However, Benko and Yu[18] succeeded in identifying the vibrational modes of the nitric oxide adducts of myoglobin, hemoglobin, and horseradish peroxidase. In this paper, we explore the use of nitric oxide to characterize the effect of substrate structure on the heme pocket of cytochrome P450cam and to provide some structural information regarding the less understood bonding interaction between iron(III) and NO in heme proteins.

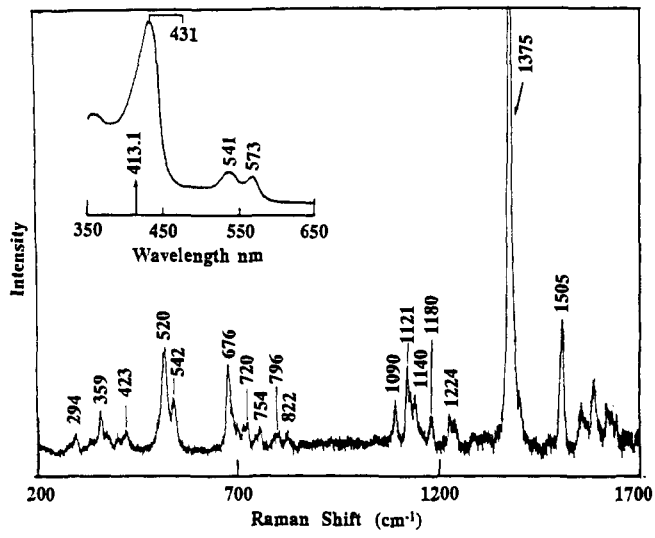

Figure 1. Soret-enhanced resonance Raman spectrum of the natural abundance nitric oxide adduct of cytochrome P450cam in the presence of saturated adamantanone. Linear backgrounds were subtracted from the spectrum in order to remove the sloping baseline. Inset shows the electronic absorption spectrum of the above-mentioned adduct. The arrow indicates the position of excitation line, 413.1 nm. No changes is found after laser illumination.

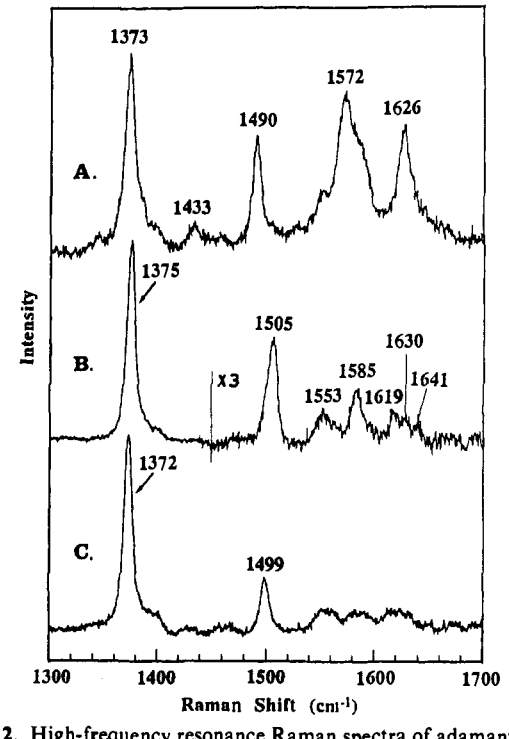

Figure 2. High-frequency resonance Raman spectra of adamantanone-bound ferric cytochrome P450cam (trace A), the ferric nitrosyl adduct (trace B), and the ferrous nitrosyl adduct (trace C).

(4) (a) Poulos, T. L.; Finzel, B. C.; Gunsalus, I. C.; Wagner, G. C.; Kraut, J. *J. Biol. Chem.* **1985**, *260*, 16122–16130. (b) Poulos, T. L.; Finzel, B. C.; Howard, A. J. *Biochemistry* **1986**, *25*, 5314. (c) Poulos, T. L.; Finzel, B. C.; Howard, A. J. *J. Mol. Biol.* **1987**, *195*, 687–700. (d) Raag, R.; Poulos, T. L. *Biochemistry* **1989**, *28*, 917–922. (e) Raag, R.; Poulos, T. L. *Biochemistry* **1989**, *28*, 7586–7592.

(5) Spiro, T. G., Ed. *Biological Applications of Raman Spectroscopy*; Vol. 3; John Wiley & Sons: New York, 1988.

(6) (a) Anzenbacher, P.; Sipal, Z.; Strauch, B.; Twardowski, J.; Proniewicz, M. *J. Am. Chem. Soc.* **1981**, *103*, 5928–5929. (b) Chottard, G.; Schappacher, M.; Ricard, L.; Weiss, R. *Inorg. Chim. Acta* **1983**, *79*, 103–104. (c) Chottard, G.; Schappacher, M.; Ricard, L.; Weiss, R. *Inorg. Chem.* **1984**, *23*, 4557–4561. (d) Anzenbacher, P.; Evangelista-Kirp, R.; Schenkman, J.; Spiro, T. G. *Inorg. Chem.* **1989**, *28*, 4491–4495.

(7) (a) Ozaki, Y.; Kitagawa, T.; Kyogoku, Y.; Shimada, H.; Iizuka, T.; Ishimura, Y. *J. Biochem.* **1976**, *80*, 1447–1457. (b) Champion, P. M.; Gunsalus, I. C.; Wagner, G. C. *J. Am. Chem. Soc.* **1978**, *100*, 3743–3751. (c) Bangchaoenpaurpong, O.; Champion, P. M.; Martinis, S. A.; Sligar, S. G. *J. Chem. Phys.* **1987**, *87*, 4273–4284.

(8) Bangchaoenpaurpong, O.; Rizos, A. K.; Champion, P. M.; Jollie, D.; Sligar, S. *J. Biol. Chem.* **1986**, *261*, 8089–8092.

(9) Champion, P. M.; Stallard, B. R.; Wagner, G. C.; Gunsalus, I. C. *J. Am. Chem. Soc.* **1982**, *104*, 5469–5472.

(10) (a) Uno, T.; Nishimura, Y.; Makino, R.; Iizuka, T.; Ishimura, Y.; Tsuboi, M. *J. Biol. Chem.* **1985**, *260*, 2023–2026. (b) Tsuboi, M. *Indian J. Pure Appl. Phys.* **1988**, *26*, 188–191.

(11) (a) Deatherage, J. F.; Maffat, K. *J. Mol. Biol.* **1979**, *134*, 401–417. (b) Piciulo, P. L.; Rupprecht, G.; Scheidt, W. R. *J. Am. Chem. Soc.* **1974**, *96*, 5293–5295. (c) Scheidt, W. R.; Frisse, M. E. *J. Am. Chem. Soc.* **1975**, *97*, 17–21. (d) Scheidt, W. R.; Piciulo, P. L. *J. Am. Chem. Soc.* **1976**, *98*, 1913–1919. (e) Scheidt, W. R.; Brinegar, A. C.; Ferro, E. B.; Kirner, J. F. *J. Am. Chem. Soc.* **1977**, *99*, 7315–7322.

(12) (a) Chien, J. C.; Dickinson, L. C. *J. Biol. Chem.* **1977**, *252*, 1331–1335. (b) Hori, H.; Ikeda-Saito, M.; Yonetani, T. *J. Biol. Chem.* **1981**, *256*, 7849–7855.

(13) Maxwell, J. C.; Caughey, W. S. *Biochemistry* **1976**, *15*, 388–396.

(14) Oosterhuis, W. T.; Lang, G. *J. Chem. Phys.* **1969**, *50*, 4381–4387.

(15) (a) Szabo, A.; Barron, L. D. *J. Am. Chem. Soc.* **1975**, *97*, 17. (b) Chottard, G.; Mansuy, D. *Biochem. Biophys. Res. Commun.* **1977**, *77*, 1333–1338. (c) Scholler, D.; Wang, M.-Y. R.; Hoffman, B. M. *J. Biol. Chem.* **1979**, *254*, 4072–4078. (d) Stong, J. D.; Burke, J. M.; Daly, P.; Wright, P.; Spiro, T. G. *J. Am. Chem. Soc.* **1980**, *102*, 5815–5819. (e) Desbois, A.; Lutz, M.; Banerjee, R. *Biochim. Biophys. Acta* **1981**, *671*, 184–192. (f) Walters, M. A.; Spiro, T. G. *Biochemistry* **1982**, *21*, 6989–6995. (g) Tsubaki, M.; Yu, N.-T. *Biochemistry* **1982**, *21*, 1140–1144. (h) Mackin, H. C.; Benko, B.; Yu, N.-T.; Gersonde, K. *FEBS Lett.* **1983**, *158*, 199–202. (i) Rousseau, D. L.; Singh, S.; Ching, Y.-C.; Sassaroli, M. *J. Biol. Chem.* **1988**, *263*, 5681–5685. (j) Han, S.; Madden, J. F.; Siegel, M.; Spiro, T. G. *Biochemistry* **1989**, *28*, 5477–5485.

(16) Waleh, A.; Ho, N.; Chantranupong, L.; Loew, G. H. *J. Am. Chem. Soc.* **1989**, *111*, 2767–2772.

(17) Saffran, W. A.; Gibson, Q. H. *J. Biol. Chem.* **1977**, *252*, 7955–7958.

(18) Benko, B.; Yu, N.-T. *Proc. Natl. Acad. Sci. U.S.A.* **1983**, *80*, 7042–7046.

Experimental Section

Cytochrome P450cam is isolated from cell paste *P. putida* (ATCC 17453), which had been grown in the presence of *d*-camphor as the only carbon source. The enzyme was purified following the procedure described by Gunsalus and Wagner,[19] with slight modifications. Highly purified enzyme solutions (RZ value of 1.5) were used throughout the experiments. Substrate camphor was removed by passage over two successive Sephadex G-25 columns. The first column had been previously equilibrated with 50 mM MOPS [2-(*N*-morpholino)propanesulfonic acid] buffer (pH ≈ 7.4) and the second with 20 mM phosphate buffer containing 100 mM of potassium chloride (pH = 7.4). The concentration of substrate (camphor or norcamphor) was 1 mM. For adamantanone-bound cytochrome P450, the substrate-free enzyme preparation was saturated with solid adamantanone in the presence of 0.2 M potassium chloride and centrifuged to remove excess solid.

The nitric oxide adducts of cytochrome P450cam were prepared by evacuating the protein solution (about 0.05 mM) in a 5-mm-o.d. NMR tube equipped with a rotationally symmetrical valve (Brunfeldt, Bartleville, OK) to remove oxygen. The tube was evacuated and filled with nitrogen at least three times. The nitric oxide was introduced to the evacuated tube through the vacuum line. Nitric oxide was cleaned by passage through a tube containing potassium hydroxide pellets before use. The sample of $^{15}N^{16}O$ (99%) was obtained from ICON Services (Summit, NJ).

Resonance Raman spectra were recorded with a Spex 1403 spectrometer equipped with a Hamamatsu R928 photomultiplier tube and a Spex DM1B system controller. The excitation beam (413.1 nm, 10 mW) was provided by a Spectra-Physics Model 100-K3 Kr^+ ion laser. The spinning 5-mm NMR tube was positioned in a backscattering geometry and was kept cooled at about 4 °C in a double-walled glass cell of in-house design by flushing with prechilled dry nitrogen gas.

Results

Addition of nitric oxide to either the substrate-bound or the substrate-free ferric cytochrome P450 results in the formation of a single, spectrally unique, species.[20] In contrast to other heme proteins, whose ferric nitrosyl complexes undergo autoreduction, the ferric nitrosyl complexes of cytochrome P450cam were quite stable at lower temperature in the absence of oxygen. We note that precipitation did occur if extreme care was not taken to remove traces of oxygen from the sample.

The RR spectrum of the ferric nitrosyl adduct of cytochrome P450cam in the presence of saturated adamantanone is displayed in Figure 1. The integrity of the sample was checked by measuring the electronic absorption spectrum before and after illumination. Since the quantum yield for photodissociation of the NO-ligated molecule is high, care was taken to monitor the spectrum for the photodissociation of bound nitric oxide and for the autoreduction of the ferric adducts. As show in Figure 2, it is found that ν_3, which occurs at 1505 cm^{-1} for the ferric NO adduct (trace B), 1499 cm^{-1} for the ferrous NO adduct (trace C), and 1490 cm^{-1} for the photodissociated species (ferric state) (trace A), is very sensitive to these changes. As can be seen in Figure 1, no evidence of a band at 1499 cm^{-1} or at 1490 cm^{-1} is detected; i.e., the RR spectrum displayed is not contaminated with either photodissociated product or the ferrous species.

The overall spectral pattern between 1300 and 1700 cm^{-1} observed for the ferric NO adduct is similar to that reported for ferric nitrosyl horseradish peroxidase.[18] It is characteristic of a six-coordinate, low-spin complex. However, careful comparison of the skeletal frequencies of these two species reveals several differences. The frequencies of modes ν_{11} and ν_3 (observed for nitrosyl cytochrome P450cam at 1553 and 1505 cm^{-1}, respectively) are lowered by about 10 cm^{-1} relative to their values for the HRP adduct. The oxidation marker band (ν_4) is also lower, but the difference is small (only 3 cm^{-1}). The difference in frequencies should reflect the variation of proximal axial ligand or heme environment. Since no difference is observed in the high-frequency region of nitrosyl complexes of cytochrome P450cam in the presence of various substrates, the later is very unlikely. It is well-known that the frequencies of porphyrin skeletal modes are correlated with the core size, which is influenced by spin state, oxidation state, back-bonding, and doming effects.[21]

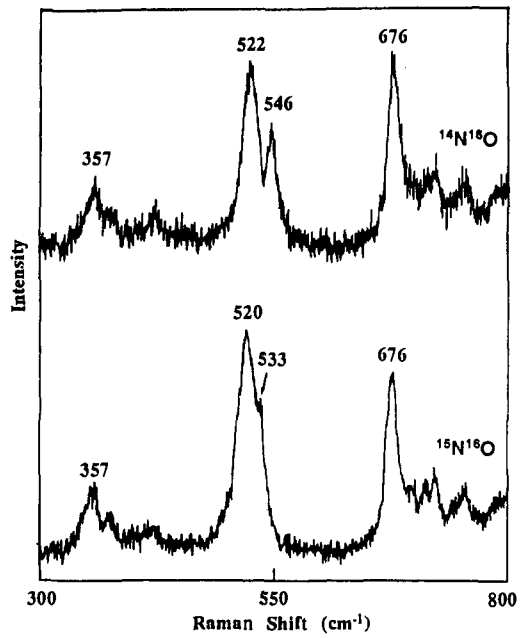

Figure 3. Low-frequency resonance Raman spectra of the ferric nitrosyl cytochrome P450cam in the presence of 1 mM camphor. The frequencies of major heme vibrational and ligand modes are labeled.

Figure 3 presents the RR spectra of the natural abundance and isotopically labeled ferric nitrosyl adduct of cytochrome P450cam in the camphor-bound form. In addition to the vibrational modes of the heme, the spectrum (upper trace) exhibits two prominent bands at 522 cm^{-1} and 546 cm^{-1}. When isotopically labeled nitric oxide ($^{15}N^{16}O$) was used to prepare the complex, the relatively strong band located at 522 cm^{-1} shifted to 520 cm^{-1} while the peak at 546 cm^{-1} shifted to 533 cm^{-1}, appearing as a shoulder on the 520 cm^{-1} feature. We assign the features at 522 cm^{-1} and 546 cm^{-1} to the stretching and bending vibrations of Fe–NO unit, respectively; noting, however, that the assignment of both modes as a mixture of bending and stretching may be more appropriate.[22]

Using Soret band excitation and three different isotopic nitric oxides ($^{14}N^{16}O$, $^{15}N^{16}O$, and $^{14}N^{18}O$), Benko and Yu[18] clearly identified the ν(Fe–NO) stretching modes at 595 cm^{-1} for ferric Mb, 594 cm^{-1} for ferric HbA, and 604 cm^{-1} for ferric HRP. These bands show 4-6 cm^{-1} downshifts upon $^{15}N^{16}O$ substitution. The bending modes of the Fe–NO unit were also located at 573 cm^{-1} for ferric Mb·NO and 574 cm^{-1} for ferric HRP·NO shifting to 562 cm^{-1} and 564 cm^{-1}, respectively, upon $^{15}N^{16}O$ substitution. Comparison of the RR spectra of cytochrome P450cam with those of the other proteins reveals two important differences. First, the enhancement of both ν(Fe–NO) and δ(Fe–N–O) in the cytochrome P450cam adducts is much stronger than that in either myoglobin or HRP. The intensity of ν(Fe–NO) in the case of cytochrome P450cam is comparable to that of the strong porphyrin mode, ν_7. In the case of the myoglobin and HRP nitrosyl complexes, this vibration is extremely weak. Second, the frequencies of these vibrational modes are substantially lower than the corresponding modes in myoglobin and HRP. The dramatic change of the observed RR spectral pattern for cytochrome P450cam compared to those of heme proteins possessing histidine as axial ligand may reflect the fundamental difference in electronic structure and therefore have important implications for biological function.

(19) Gunsalus, I. C.; Wagner, G. C. *Methods Enzymol.* **1978**, *52*, 166–188.

(20) O'Keeffe, D. H.; Ebel, R. E.; Peterson, J. A. *J. Biol. Chem.* **1978**, *253*, 3509–3516.

(21) (a) Spaulding, L. D.; Cheng, C. C.; Yu, N.-T.; Felton, R. H. *J. Am. Chem. Soc.* **1975**, *97*, 2517. (b) Spiro, T. G.; Strong, J. D.; Stein, P. *J. Am. Chem. Soc.* **1979**, *101*, 2648. (c) Choi, S.; Lee, J. J.; Wei, Y. H.; Spiro, T. G. *J. Am. Chem. Soc.* **1983**, *105*, 3692–3707. (d) Parthasarathi, N.; Hanson, C.; Yamaguchi, S.; Spiro, T. G. *J. Am. Chem. Soc.* **1987**, *109*, 3865.

(22) Li, X. Y.; Spiro, T. G. *J. Am. Chem. Soc.* **1988**, *110*, 6024–6033.

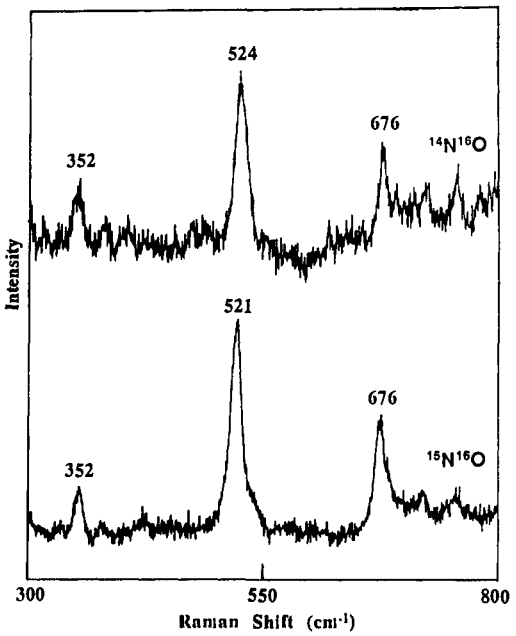

Figure 4. Low-frequency RR spectra of the ferric nitrosyl cytochrome P450cam in the presence of 1 mM norcamphor.

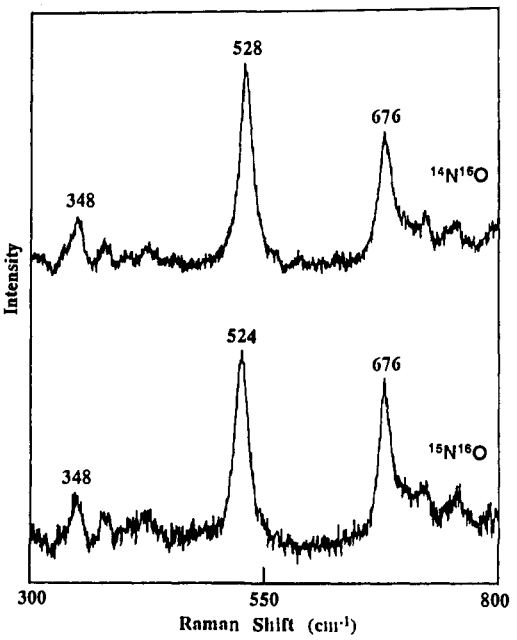

Figure 5. Low-frequency RR spectra of the nitric oxide adduct of substrate-free cytochrome P450cam.

Figures 4 and 5 present the RR spectra of ferric nitrosyl complexes of cytochrome P450cam in the presence of norcamphor, a camphor analogue of smaller size, and in the absence of substrate, respectively. Essentially different spectral patterns from that observed for the camphor-bound derivative are exhibited. First, the band located at 546 cm^{-1} in the camphor-bound nitrosyl cytochrome P450cam is absent in both spectra. Also, the feature located at 522 cm^{-1} in the case of the camphor-bound form is shifted to 528 cm^{-1} in the substrate-free complex (Figure 5). The RR spectra of the nitrosyl adduct of the enzyme in the norcamphor-bound state, shown in Figure 4, is very similar to Figure 5. However, the intense band appears at 524 cm^{-1}, i.e., at an intermediate frequency. The isotopic sensitivity of these two bands confirms their assignment as ν(Fe–NO).

Careful comparison of the spectra shown in Figures 1–5 reveals another substrate-sensitive band of medium intensity, which occurs at 357 cm^{-1} in camphor-bound ferric nitrosyl cytochrome P450cam and shifts to 349 cm^{-1} when camphor is removed. For the norcamphor and adamantanone bound nitrosyl complexes, this band was observed at 352 and 359 cm^{-1}, respectively. Although carbon monoxide complexes of ferrous cytochrome P450cam are expected to have the same geometry as that of ferric nitrosyl complexes, their Raman spectra do not show this kind of substrate-dependent band. Since the vibrational frequency of this mode is very close to the Fe–S stretching frequency identified by RR for ferric high-spin cytochrome P450cam[9] and by infrared spectroscopy for a series of model compounds,[23] we tentatively assign this mode to Fe–S stretching. The distortion of the Fe(III)–NO linkage by substrates results in the weakening of the Fe(III)–NO bond. This should be compensated by the strengthening of the Fe–S bond. The experimental results are clearly consistent with this expected trend. When the environment of heme pocket is changed from empty to adamantanone, the ν(Fe–NO) decreases from 528 to 520 cm^{-1}, while the ν(Fe–S) increases from 349 to 359 cm^{-1}.

Table I. Resonance Raman Data (cm^{-1}) of the Isoelectronic Adducts of the Ferric Nitrosyl Fragment

molecules	ν(M–XO)	δ(MXO)	ν(X–O)	ref
(cytochrome)Fe^{III}–NO				
adamantanone	520	542		*a*
camphor	522	546		*a*
norcamphor	524			*a*
substrate free	528			*a*
(Mb)Fe^{III}–NO	595	573		18
(HRP)Fe^{III}–NO	604	574		18
(HbA)Fe^{III}–NO	594			18
(Hb)Mn^{II}–NO	623	573	1721	25
(Mb)Mn^{II}–NO	627	574	1713	25
(pip)PPPDMe)Mn^{II}–NO	627	566	1735	33
(CCTIXHb)Mn^{II}–NO	628	574	1735	32
(NMI)(Heme-5)Mn^{II}–NO	629		1736	33
(NMI)(SP-15)Mn^{II}–NO	631	578	1727	33
(NMI)(SP-14)Mn^{II}–NO	632	575	1718	33
(Cyt P450cam)Fe^{II}–CO				
adamantanone	474			10
camphor	481	558	1940	10
norcamphor	473			10
substrate free	464		1963	10
(sperm whale Mb)Fe^{II}–CO	512	577	1955	48
(HbA)Fe^{II}–CO	507	578	1951	48

[a] This work.

Discussion

A. Strong Electron Donation of Cysteinyl Sulfur. The ferric nitrosyl adduct is isoelectronic with the ferrous carbonmonoxy complex of heme proteins and the nitrosyl adducts of manganese(II)-substituted heme proteins, having a total of six electrons in the metal d and ligand π^* orbitals. A linear Fe–NO linkage is expected, based on X-ray crystallography data for compounds lacking distal steric effects.[24] The local vibrational data for these isoelectronic molecules are summarized in Table I, which includes the present and previous experimental work. It is interesting to compare the vibrational modes ν(M–XO) and δ(M–X–O) for the various adducts. The frequencies of the bending modes are very similar, but the stretching frequencies differ by 160 cm^{-1} among the isoelectronic molecules, the implied large difference in bond strength being readily explained by the π-bonding scheme.[25]

A change in the nature of the axial ligand can have a great influence on the vibrations of the M–X–O unit. The ν(Fe–CO) frequencies of the model compounds, Fe(T_{piv}PP)CO-L, were observed at 486, 489, 496, and 527 cm^{-1} for L = py, 1-MeIm, 1,2-diMeIm, and THF, respectively.[26] The results suggest that a weaker Fe(II)–L bond at the trans position gives rise to a stronger Fe–CO bond. When L is $C_6F_5S^-$, the ν(Fe–CO) is observed at 479 cm^{-1}, i.e., somewhat lower than that of corresponding compounds with axial ligands containing oxygen or

(23) Oshio, H.; Ama, T.; Watanabe, T.; Nakamoto, K. *Inorg. Chem. Acta* **1985**, *96*, 61–66.
(24) Scheidt, W. R.; Lee, Y. J.; Hatano, K. *J. Am. Chem. Soc.* **1984**, *106*, 3191–3198.
(25) Parthasarathi, N.; Spiro, T. G. *Inorg. Chem.* **1987**, *26*, 2280–2282.
(26) Kerr, E. A.; Mackin, H. C.; Yu, N.-T. *Biochemistry* **1983**, *22*, 4373–4379.

nitrogen donor atoms.[6b] The RS^- anion (bound trans to CO) is a good donor, inducing a weakening of the bonding of CO to iron, as reflected by a decrease in ν(Fe–CO). This drastic weakening of Fe–CO bonding was also observed for various ferrous carbonyl cytochromes P450. The stretching frequency ν(Fe–CO) found at 481 cm^{-1} for cytochrome P450cam,[10a] 477 cm^{-1} for cytochrome P450 from bovine adrenocoricul mitochondria,[27] and 474 cm^{-1} for microsomal cytochrome P450(RLM3),[6d] is about 30 cm^{-1} lower than that observed for myoglobin and hemoglobin.

Interestingly, this marked weakening of the iron–ligand bond in cytochrome P450 is magnified in the case of ferric nitrosyl complexes of cytochrome P450cam. The stretching frequency of Fe–NO is about 80 cm^{-1} down-shifted compared to that of heme proteins possessing histidyl imidazole as the axial ligand. Nitric oxide is bound to ferric heme iron through σ and π interactions both interactions determining the strength of the Fe–NO bond. On the other side of heme iron, a cysteinyl thiolate anion (S^-) has two pairs of electrons available for bonding (i.e., $3p_y$ and $3p_z$). It can bind to the heme iron through a $3p_y$–d_π interaction (π bonding) as well as a $3p_z$–d_{z^2} interaction (σ bonding). For the heme proteins possessing imidazole as the axial ligand, this bonding scheme is also operative, but the extra pair of electrons for π bonding and the negative charge on the thiolate sulfur make it an unusual axial ligand with much better σ and π donor ability. The consequences are clearly reflected in the weakening of Fe–CO and Fe–NO in cytochrome P450cam complexes.

B. Linear or Bent Structure for the Fe–N–O Linkage. It is known that the intrinsic geometry of the M–X–Y linkage in hemeproteins and metalloporphyrins depends on the total count of electrons on the d orbital of the central metal and on the π^* or σ^* orbitals of the bound X–Y molecule. The M–X–Y linkage changes from linear to bent if the total electron count approaches seven and becomes more bent as more electrons are introduced to the MXY fragment. This empirical observation is strongly supported by theoretical calculations[28] and structural determinations of many transition-metal complexes containing diatomic ligands.[29] A well-known example is the nitric oxide adduct of ferrous TPP, for which the addition of one electron to the linear six-electron, ferric nitrosyl TPP adduct drives the ∠FeNO to 140°.[11]

Considering the strong electron donating effect of cysteinyl sulfur observed in the present and previous studies, it may be argued that the ferric NO unit of cytochrome P450cam cannot be considered as a six-electron system. Rather, the thiolate axial ligand may effectively donate an electron to make the ferric NO fragment closer to a seven-electron system, which implies a substantially bent geometry for the Fe–N–O linkage. However, as is discussed below, consideration of the present results, in terms of the vibrational characteristics of the relevant bent MXY systems, suggest that the Fe–N–O linkage is essentially linear in the NO adduct of ferric cytochrome P450cam in the absence of substrate.

In the Soret-excited RR spectra of the carbon monoxide adducts of heme proteins, two low-frequency modes assignable to the stretching and bending vibrations of the FeCO fragment are frequently observed and identified through their characteristic isotope-shifting pattern.[30] However, for simple heme adducts (i.e., except for strapped heme[31]), only the stretching mode has been observed. These observations led Yu and co-workers to suggest that the enhancement of the bending mode is indicative of off-axis binding, the intensity being taken as a measure of the degree of distortion.[31] They also proposed an activation mechanism that involves the tilting of the FeCO linkage. This mechanism was further extended by Li and Spiro[22] to include the asymmetrical electronic influence in the vicinity of the bound CO. The RR study of the CO adduct of cytochrome P450cam provides a test case. The bending mode was observed with moderate intensity in the presence of camphor but became undetectable upon the removal of substrate. It is conceivable that the steric bulk of camphor distorts the FeCO structure, thus providing an effective activation route for enhancement of the bending mode.

The isoelectronic analogues, the NO adduct of Mn(II)-substituted proteins, also exhibit a similar enhancement pattern for the ν(Mn–NO) and δ(Mn–N–O) modes. For the nitric oxide adducts of manganese-reconstituted myoglobin, hemoglobin,[25] and CCT-IX hemoglobin,[32] the ν(Mn–NO) and δ(Mn–N–O) vibrations were simultaneously observed at ~625 cm^{-1} and ~574 cm^{-1}, respectively. Further studies employing strapped hemes revealed the presence of a distorted MnNO linkage, thus accounting for enhancement of the bending mode.[33] However, Yu and co-workers also demonstrated that the bending mode can be activated by introducing an asymmetrical base in the unstrained model compounds.[33]

In brief, careful studies of linear diatomic XY adducts of heme proteins and model compounds support the conclusion that the lack of the enhancement of the bending mode is an indication of a linear FeXY fragment. On the other hand, the simultaneous observation of both the stretching and bending vibrations does not *necessarily* confirm the presence of a bent or tilted FeXY unit, since other activation mechanisms may be responsible for the enhancement.[33]

The essential issue concerns the expected vibrational pattern for a bent FeNO linkage. To this end, we first analyze the available vibrational data for the $Fe–O_2$ unit, whose vibrations are the better understood among the bent MXY molecules. Brunner[34] first observed a band 567 cm^{-1} in the 514.7-nm excited Raman spectra of oxyhemoglobin and assigned it to $\nu(Fe–O_2)$. However, Benko and Yu[18] found this mode was virtually insensitive to isotopic substitution of the outer oxygen atom and reassigned it to $\delta(Fe–O_2)$. The dispute was resolved by a normal coordinate simulation of the two observed isotope-sensitive bands for oxygenated ferrous phthallocyanine in an oxygen matrix at 15 K by Nakamoto and co-workers,[35] who supported Brunner's original assignment. Recently, we[36] have also detected the bending mode of oxyhemoglobin, which downshifts from 426 to 413 cm^{-1} upon $^{16}O_2/^{18}O_2$ substitution. In a relevant dioxygen adduct of cobalt-reconstituted hemoglobin, Yu et al.[37] identified two oxygen isotope sensitive bands that are assignable to the stretching (537 cm^{-1}) and bending (390 cm^{-1}) vibrations.

For the nitric oxide adduct of ferrous hemeproteins, which are seven-electron systems and the turning point along the effect of total electron count on the linkage geometry, the detection and assignment of the expected vibrational modes have long been a controversial issue.[15] However, we[38] recently succeeded in observing two isotope-sensitive lines in the low-frequency RR spectra of nitrosyl ferrous cytochrome P450cam, myoglobin, and hemoglobin by using multiple isotope labeling of the NO molecule. For the myoglobin adduct, the stretching modes occur at 554 ($^{14}N^{16}O$), 546 ($^{15}N^{16}O$), 552 ($^{14}N^{18}O$), and 542 ($^{15}N^{18}O$) cm^{-1}, while the bendings are observed at 449 ($^{14}N^{16}O$), 447 ($^{15}N^{16}O$), 445 ($^{14}N^{18}O$), and 443 ($^{15}N^{18}O$) cm^{-1}.

In conclusion, an intrinsically bent MXY system is expected to give rise to two observed modes in the low-frequency region, both of which should be detected in the absence of accidental overlapping with macrocycle modes. Inasmuch as the spectrum

(27) Tsubaki, M.; Ichikawa, Y. *Biochim. Biophys. Acta* **1985**, *827*, 268–272.
(28) (a) Hoffmann, R.; Chen, M. M.-L.; Thorn, D. L. *Inorg. Chem.* **1977**, *16*, 503–511. (b) Mingos, D. M. P. *Inorg. Chem.* **1973**, *12*, 1209–1211.
(29) (a) Feltham, R. D.; Enemark, J. H. *Top. Stereochem.* **1981**, *12*, 155. (b) Enemark, J. H.; Feltham, R. D. *Coord. Chem. Rev.* **1974**, *13*, 339.
(30) (a) Kerr, E. A.; Yu, N.-T. In *Biological Applications of Raman Spectroscopy*; Spiro, T. G., Ed.; Wiley & Sons: New York, 1988. (b) Yu, N.-T. *Methods Enzymol.* **1986**, *130*, 350–409.
(31) Yu, N.-T.; Kerr, E. A.; Ward, B.; Chang, C. K. *Biochemistry* **1983**, *22*, 4534.
(32) Lin, S. H.; Yu, N.-T.; Gersonde, K. *FEBS Lett.* **1988**, *229*, 367–371.
(33) Yu, N.-T.; Lin, S. H.; Chang, C. K.; Gersonde, K. *Biophys. J.* **1989**, *55*, 1137–1144.
(34) Brunner, H. *Naturwissenschaften* **1974**, *61*, 129.
(35) Bajdor, K.; Oshio, H.; Nakamoto, K. *J. Am. Chem. Soc.* **1984**, *106*, 7273–7274.
(36) Jeyarajah, S. Ph.D. Thesis, Marquette University, 1990.
(37) Thompson, H. M.; Yu, N.-T.; Gersonde, K. *Biophys. J.* **1987**, *51*, 289–295.
(38) Hu, S.; Kincaid, J. R., manuscript in preparation.

of cytochrome P450cam is relatively uncongested in this region, the vibrational behavior for the substrate-free enzyme is inconsistent with a bent FeNO fragment.

We now return our attention to the ferric NO adducts of heme proteins. In the low-frequency RR spectra of ferric nitrosyl myoglobin, hemoglobin, and horseradish peroxidase, Benko and Yu[18] observed two isotope-sensitive bands at 595 and 573 cm^{-1}, one exhibiting a monotonous (595 cm^{-1}) and the other a zigzag (573 cm^{-1}) isotope-shifting pattern. These two modes were assigned to the stretching and bending vibrations, accordingly. It is not surprising that the bending mode is enhanced in these cases, considering the fact that the corresponding modes for the CO adducts of these proteins were also enhanced.

Our present study of the NO adduct of ferric cytochrome P450cam in the presence of various substrates permits an assessment of steric effects on the vibrations of this system. As discussed previously, the stretching mode is very sensitive to the size of substrate analogues, the effect being proportional to the steric strain imposed on the bound NO. Of particular interest is the considerable intensity of the bending mode in the RR spectra of the adamantanone- and camphor-bound adducts. This mode is completely absent in the substrate-free form. This enhancement pattern of the bending vibration is similar to that of the FeCO fragment in the carbon monoxide adducts of cytochrome P450cam[10a] and P450scc[39] in the presence of their respective substrates. Thus, the vibrational behavior of the FeNO unit in the cytochrome P450cam adducts, as revealed in this work, is similar to those of a linear MXY linkage such as FeCO and MnNO moieties.

C. Effects of Substrates on the Vibrations of the M–X–O Unit. An interesting aspect of cytochrome P450cam is the effect of substrate on the heme active site. The binding of substrates controls the spin state,[40] redox potential of the heme iron,[41] and the ligand affinity of the ferrous enzyme for carbon monoxide.[42] The substrate, camphor, is also known to greatly stabilize the inherently unstable oxygenated complexes.[43] Although the electronic absorption spectra of the carbon monoxide adducts of cytochrome P450cam, with and without substrate present, show no detectable difference, RR spectroscopy was used to detect a subtle difference in structure.[10] The intense line at 481 cm^{-1}, assignable to ν(Fe–CO) of the FeCO fragment of camphor-bound P450cam, shifts to 464 cm^{-1} upon the removal of substrate. A similar effect was observed by RR studies[39] for the CO complexes of cytochrome P450scc with different substrates.

From the RR studies of the CO and NO adducts of cytochrome P450cam, it is clear that the substrate or analogues perturb the heme pocket and the bound diatomic ligands, as reflected in the observed vibrational modes. The frequency perturbation results from the combined influence of an electronic factor, which determines the strength of the M–XY linkage and the kinematic effect, which arises from the distortion of the M–XY fragment. In order to understand the observed spectral pattern, it is necessary to analyze the expected vibrational consequences of the distortion-induced electronic and kinematic effects.

1. Kinematic Effect. In order to test the assignment of the observed vibrational modes and to examine the origin of the effect of substrate structure on the local vibrations of axial ligands in nitrosyl cytochrome P450cam, we have carried out a normal coordinate analysis on a tetratomic L–Fe–N–O system (L stands for CH_3S with a dynamic mass, 47 amu). The structural parameters adopted from the crystallographically determined geometry of the nitric oxide adduct of a ferric porphyrin[24] are as follows: d(Fe–N) = 1.74 Å, d(N–O) = 1.10 Å, d(Fe–L) = 2.40 Å, ∠Fe–N–O = 180°, and ∠L–Fe–N = 180°. d(Fe–L) is taken from the crystallographic data of the CO adduct of cytochrome P450cam.[4e] The force constants used in the calculation for stretching modes are K(N–O) = 10.5, K(Fe–N) = 3.15, and K(Fe–L) = 2.4 mdyn/Å. For bending, the constants are H(Fe–N–O) = 0.78 and H(L–Fe–N) = 0.35 mdyn·Å. The stretch–stretch interaction constants between two adjacent bonds are k(L–Fe,Fe–N) = 0.25 and k(Fe–N,N–O) = 0.2 mdyn/Å. The frequencies of the normal modes, calculated with the use of Schachtschneider and Mortimer's programs[44] (CART, GMAT, and VSEC), are ν(N–O) = 1600 cm^{-1}, δ(Fe–N–O) = 528 cm^{-1}, ν(Fe–NO) = 547 cm^{-1}, and ν(Fe–S) = 349 cm^{-1}. The isotopic ($^{15}N^{16}O$) shifts for bending (14 cm^{-1}) and stretching (3 cm^{-1}) agree well with the observed values. Where the ν(N–O) was not experimentally observed, when K(N–O) is varied between 10.0 and 11.0 mdyn/Å, the effects on ν(Fe–NO) and δ(Fe–N–O) were found to be negligible in our calculation. Based on this set of force constants, we now investigate the kinematic effect of bending and tilting of the Fe–N–O structure on the vibrational modes.

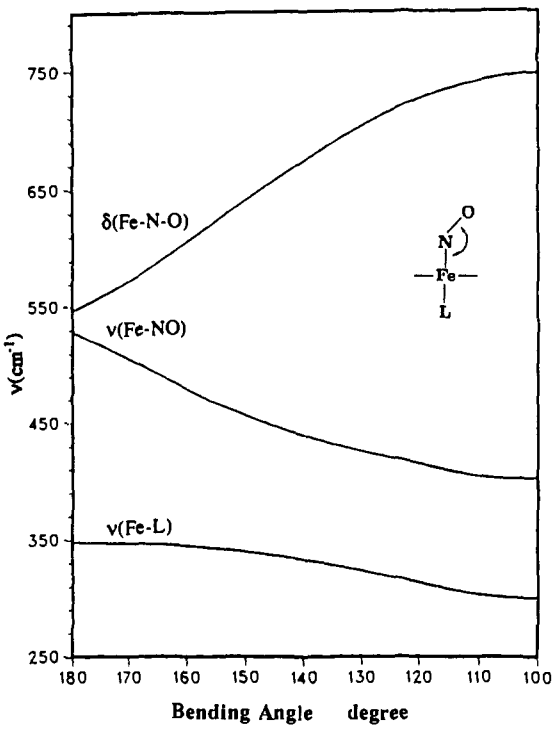

Figure 6. Plots of the calculated frequencies of the δ(Fe–N–O), ν(Fe–NO), and ν(Fe–L) modes as a function of the Fe–N–O angle. The force constants are given in the text.

Bending. As revealed by X-ray structural determinations[4a-d] of cytochrome P450cam (in the absence and presence of substrate and analogues), the introduction of a substrate into the active site makes the heme pocket narrower for the bound ligand, thus forcing it to distort to release the imposed strain. In the carbon monoxide adduct,[4e] the ∠Fe–C–O was found to be 168°, but for the nitric oxide adduct, little is known about the possible distortion. However, an X-ray crystallographic study of ferric nitrosyl cytochrome c peroxidase[45] indicates a substantially bent structure. Accordingly, we examined the vibrational consequence of this kind of geometrical distortion of bound nitric oxide. In Figure 6, the calculated vibrational frequencies are plotted as a function of Fe–N–O angle, with the force constant values remaining the same

(39) Tsubak, M.; Hiwatashi, A.; Ichikawa, Y. *Biochemistry* **1987**, *26*, 4535–4540.
(40) (a) Sligar, S. G. *Biochemistry* **1976**, *15*, 5399–5406. (b) Fisher, M. T.; Sligar, S. G. *J. Am. Chem. Soc.* **1985**, *107*, 5108.
(41) Sligar, S. G.; Gunsalus, I. C. *Proc. Natl. Acad. Sci. U.S.A.* **1976**, *73*, 1078–1082.
(42) Peterson, J. A.; Griffin, B. W. *Arch. Biochem. Biophys.* **1972**, *151*, 427–433.
(43) (a) Ishimura, Y.; Ullrich, V.; Peterson, J. A. *Biochem. Biophys. Res. Commun.* **1971**, *42*, 147–153. (b) Lipscomb, J. D.; Sligar, S. G.; Namtvedt, M. J.; Gunsalus, I. C. *J. Biol. Chem.* **1976**, *251*, 1116–1124. (c) Debey, P.; Balny, C.; Douzou, P. *FEBS Lett.* **1976**, *69*, 231–235, 236–239. (d) Eisenstein, L.; Debey, P.; Douzou, P. *Biochem. Biophys. Res. Commun.* **1977**, *77*, 1377–1383.
(44) Schachtschneider, J. H.; Mortimer, F. S. *Vibrational Analysis of Polyatomic Molecules*; Technical Reports No 231–61; Shell Development Co.: Emeryville, CA, 1964.
(45) (a) Edwards, S. L.; Kraut, J.; Poulos, T. L. *Biochemistry* **1988**, *27*, 8074–8081. (b) Edwards, S. L.; Poulos, T. L. *J. Biol. Chem.* **1990**, *265*, 2588–2595.

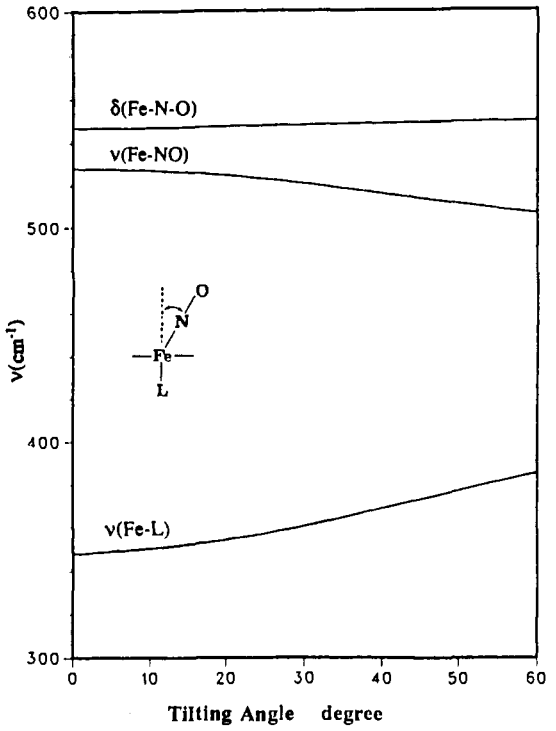

Figure 7. Plots of the calculated frequencies of the δ(Fe–N–O), ν(Fe–NO), and ν(Fe–L) modes as a function of the tilt angle, as defined in the figure. The force constants are the same as those given in the text.

as those of the linear model. As the Fe–N–O angle decreases, ν(Fe–NO) decreases and δ(Fe–N–O) increases. The calculated ν(Fe–S) also decreases steadily.

Tilting. Figure 7 represents the kinematic effect on the axial vibrations of a different geometrical distortion; i.e., tilting of NO from the normal of the heme plane. The calculation shows a slight decrease in ν(Fe–NO) and increase in ν(Fe–S) with the tilting of the NO group. The δ(Fe–N–O) mode is very weakly dependent on tilting.

2. Electronic Factor. The bonding strength and geometry of the M–XY linkage in general are primarily determined by two types of bonding between the transition metal and the diatomic ligand, i.e., σ bonding and π bonding. The σ bonding is derived from the overlap of the metal d_{z^2} orbital and the ligand n orbital (or one of the π^* orbitals for the bent molecules). The π bonding is due to the interaction of the metal d_{xy} and d_{yz} with the ligand π^* orbitals. In addition, the competition for the d_π electron density between the antibonding π^* orbitals of both the porphyrin and the XY molecule also plays an important role.

The nature of the bonding in transition-metal nitrosyl complexes has been studied intensely by Hoffmann and co-workers and Mingos[28] in their theoretical calculations. From the constructed Walsh diagrams, it can be seen that two interactions dominate the bending process. As the nitrosyl bends, the bonding π orbital (d_{xy}–π^*) mixes strongly with the antibonding σ orbital (d_{z^2}–n), resulting a sharp increase in the antibonding character of the bonding π orbital. This effect will lead to a substantially decreased π back-bonding. On the other hand, the increase in the bonding character of the d_{z^2}–n orbital would favor the σ bonding of the d_{z^2} orbital with the trans ligand. The net result will be weaker M–XY and stronger M–L bonding.

For the tilting distortion, there would be little bonding change between the transition metal and the bound diatomic ligand, except for the competition for the d_π electron of the central metal between the π^* orbitals of the XY molecule and the porphyrin ring. As outlined by Li and Spiro,[22] the net result is a decreased Fe–porphyrin back-bonding and, consequently, an enhanced Fe–XY back-bonding, owing to the misalignment of the iron and porphyrin π orbitals. It is conceivable that the reorientation of the Fe orbital toward the linear FeNO unit will lead to a poorer overlap of the Fe d_{z^2} orbital and the p_z orbital of the trans cysteinyl sulfur, thus weakening the Fe–S bonding.

Based on these principles, we now propose an explanation for the simultaneous weakening of Fe(III)–NO bonding and the strengthening of the Fe–S bonding upon the introduction of substrate to the heme pocket. Although the calculated results of the tilting scheme would fit the experimental observations [i.e., lowering of the ν(Fe–NO) and increasing of the ν(Fe–S) mode], the small frequency change could be easily offset by the accompanying increase of the related force constant, K(Fe–N), and corresponding decrease of K(Fe–S). Both effects are expected from the consideration of the σ–π bonding scheme discussed above. A plausible explanation is that the Fe–NO unit adopts a linear linkage in the substrate-free adduct and becomes bent in the presence of substrate. For the ν(Fe–NO) mode, both the kinematic and electronic effects are in the same direction, i.e., lowering of the frequency as the steric strain imposed by substrates becomes larger. Although the vibrational analysis predicts a small decrease in ν(Fe–S) (Figure 6) in a bent FeNO configuration, the bending process will substantially push up the wavenumber of the ν(Fe–S) mode by reinforcing the Fe–S bonding. The net result is the small frequency increase in the ν(Fe–S) vibration.

3. Comparison between the Vibrational Pattern of the Fe(III)–NO and the Fe(II)–CO Unit. It is interesting to compare the vibrational behavior of the Fe–X–O frequencies in the ferrous–CO and ferric–NO adducts as a function of substrate size. In the case of the CO adducts, ν(Fe–CO) was observed at 464 cm^{-1} for the substrate-free form and 481 cm^{-1} for the camphor-bound analogue. An intermediate frequency (473 cm^{-1}) is observed when norcamphor (a substrate of smaller size than camphor) is employed as substrate. In the case of adamantanone, ν(Fe–CO) is observed at 474 cm^{-1}, a frequency that is essentially indistinguishable from that of the norcamphor derivative. This is unexpected inasmuch as the larger steric bulk of adamantanone may be expected to lead to a greater degree of distortion of the FeCO fragment. Indeed, recent X-ray crystallographic studies[4d] clearly demonstrate that adamantanone occupies a position within the active site that is similar to that of camphor, whereas norcamphor binds about 0.9 Å further away from the oxygen binding site. The data presented here for the NO adducts is consistent with the crystallographic results. Thus, an isolated ν(Fe–NO) is observed at 528 cm^{-1} in the absence of substrate (Figure 5). For the small substrate norcamphor, the isolated ν(Fe–NO) occurs at 524 cm^{-1}. The two large substrates (camphor and adamantanone) give rise to the doublet structure show in Figures 1 and 3.

Finally, we note here that the local distortion of the isoelectronic Fe(II)–CO and Fe(III)–NO linkages by various substrates in cytochrome P450cam results in opposite trends in the frequency change of the Fe–XO stretching mode. For the carbon monoxide adducts, the steric hindrance causes the ν(Fe–CO) frequency to increase as observed for both the enzyme[10a] and the strapped porphyrins.[31] It was suggested[10] that the substrate, when bound, causes steric hindrance of the CO bonding site and forces the FeCO grouping to bend away from the normal 180°. However, the vibrational analysis made by Li and Spiro[22] suggests that a substantially bent structure is very unlikely for the carbonyl heme proteins. It is likely that the observed strengthening of the Fe–CO bonding is due to the enhanced Fe→CO back-donation induced by the tilting of the Fe–CO linkage and this effect will offset the small kinematic decrease of the ν(Fe–CO) mode arising from such a distortion coordinate. On the other hand, a bending distortion of the FeNO fragment, induced by a steric factor, leads to a substantial decrease on the ν(Fe–NO) frequency.

We attribute the difference in the distortion coordinate of the Fe–XO linkages between CO and NO adducts upon the subjection to steric hindrance to the different strengths of the metal d_{z^2}–ligand π^* orbital interaction, a factor that is governed by the energy of the π^* orbital of the free ligand. The calculation carried out by Mingos[28b] suggests that this interaction is much stronger in the nitrosyl complexes than in the carbonyl adducts, owing to the well-matched energies of the metal d_{z^2} and NO π^* orbitals. Similar arguments also justify the interpretation of the RR spectra

of the CN^- adducts of myoloperoxidase, horseradish peroxidase,[46] and sulfite reductase.[15j] We wish to point out that a bent FeCN structure will lead to an observed downshift of ν(Fe–CN) mode for the cyanide adducts of sterically hindered hemes.[47]

Summary

The resonance Raman spectra of the nitric oxide adducts of cytochrome P450cam in several substrate-bound forms are reported. These adducts are formulated as six-coordinate, low-spin compounds. The ν(Fe–NO) and δ(Fe–NO) modes are detected and assigned through isotopic substitution and found to be dramatically lower than those of the corresponding myoglobin and horseradish peroxidase adducts. On the basis of a consideration of both electronic and kinematic factors, the effect of the substrate structure on the metal–ligand vibrations can be explained by adopting a slightly bent geometry of the intrinsically linear Fe–NO linkage in the substrate-bound form.

Acknowledgment. This work was supported by a grant from the National Institute of Health (DK35153 to J.R.K.).

(46) Lopez-Garriga, J. J.; Oertling, W. A.; Kean, R. T.; Hoogland, H.; Wever, R.; Babcock, G. T. *Biochemistry* **1990**, *29*, 9387-9395.
(47) Tanaka, T.; Yu, N.-T.; Chang, C. K. *Biophys. J.* **1987**, *52*, 801-805.
(48) Tsubaki, M.; Srivastava, R. B.; Yu, N.-T. *Biochemistry* **1982**, 1132.

Investigation of the Kinetic Window for Generation of ^{13}C T_0–S CIDNP Derived from Long-Chain Biradicals by Tuning the Rates of Bimolecular Scavenging and Intersystem Crossing

Kuo Chu Hwang, Nicholas J. Turro,* and Charles Doubleday, Jr.*

Contribution from the Department of Chemistry, Columbia University, New York, New York 10027. *Received June 13, 1990*

Abstract: In the absence of radical scavengers, the products of biradicals generated from photolysis of 2-phenylcycloalkanones exhibit no CIDNP. Addition of a radical scavenger such as CCl_4 or $CBrCl_3$ gives rise to strong CIDNP derived from T_0–S intersystem crossing. The CIDNP intensity depends on the scavenger concentration, the molecular chain length of the biradical, and the reaction temperature. The results are interpreted in terms of a simple kinetic scheme which implies a kinetic window within which T_0–S CIDNP is efficiently generated in biradicals. Bimolecular scavenging is sufficient to provide the strong competition with intersystem crossing needed to produce T_0–S CIDNP. From a knowledge of the dependence of CIDNP intensity on scavenger concentration and the previously measured biradical lifetimes, the rate constant of halogen atom abstraction by the acyl radical moiety is estimated to be 1×10^6 M^{-1} s^{-1} for Cl abstraction from CCl_4 and 1×10^9 M^{-1} s^{-1} for Br abstraction from $CBrCl_3$.

Introduction

In radical pairs, CIDNP is usually generated by intersystem crossing (ISC) between the middle triplet level T_0 and the singlet state S. Two things normally prevent T_0–S CIDNP from being observed in biradicals. First, biradicals have a significant singlet–triplet energy gap ΔE_{ST} that arises from the radical centers being connected together so they cannot diffuse farther apart than the chain permits. If ΔE_{ST} is much larger than the electron–nuclear hyperfine coupling (HFC), T_0–S ISC is inefficient and CIDNP is dominated by the interaction of S with one of the $T_{\pm 1}$ levels, usually T_{-1}. Generally this means that T_0–S CIDNP is found only in long-chain biradicals, because ΔE_{ST} decreases exponentially with increasing end-to-end distance in the biradical.[1] Second, even if ΔE_{ST} is small enough, there must be a process competing with HFC which is independent of nuclear spin and leads to different products. If all mechanisms of biradical decay yield the same product distribution, T_0–S CIDNP cannot be produced because the total number of α and β nuclear spins in the products is not changed by T_0–S ISC. In radical pairs the competing process is usually diffusive separation of the radicals.[2] Other possible competitive processes are spin–lattice relaxation,[3a] formation of triplet excited state products,[3b] spin–orbit coupling in biradicals,[3c,d] and bimolecular radical scavenging of biradicals.[4] Kaptein showed that bimolecular scavenging of biradicals by radical scavengers can produce T_0–S CIDNP in the scavenging products, whose CIDNP resembles that of cage-escape products in ordinary radical pair CIDNP.[4] More recently, we have observed[5] that long-chain flexible biradicals generated from photolysis of 2-phenylcycloalkanones give no photo-CIDNP unless a bimolecular scavenging reaction provides a competition which allows T_0–S CIDNP to be generated. The maximum CIDNP signals are generated when the scavenging rate is comparable to the ISC rate.[5] This "kinetic window" for production of T_0–S CIDNP is

Scheme I. Photoreaction of 2-Phenylcyclododecanone

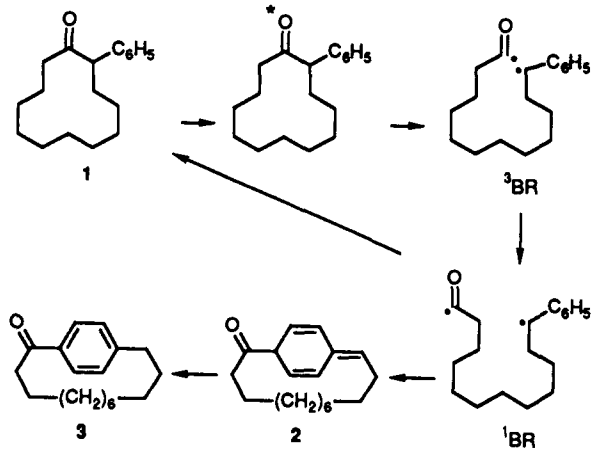

(1) DeKanter, F. J. J.; denHollander, J.; Huizer, A.; Kaptein, R. *Mol. Phys.* **1977**, *34*, 857.
(2) (a) *Chemically Induced Magnetic Polarization*; Lepley, A. R., Closs, G. L., Eds.; Wiley and Sons: New York, 1973. (b) *Spin Polarization and Magnetic Effects in Radical Reactions*; Molin, Yu. N., Ed; Elsevier: Amsterdam, 1984.
(3) (a) Hutton, R. S.; Roth, H. D.; Kraeutler, B.; Cherry, W. R.; Turro, N. J. *J. Am. Chem. Soc.* **1979**, *101*, 2227. (b) Roth, H. D.; Manion-Schilling, M. L. *J. Am. Chem. Soc.* **1980**, *102*, 4303. (c) Doubleday, C., Jr. *Chem. Phys. Lett.* **1979**, *64*, 67; **1981**, *79*, 375. (d) DeKanter, F.; Kaptein, R. *J. Am. Chem. Soc.* **1982**, *104*, 4759.
(4) DeKanter, F. J. J.; Kaptein, R. *Chem. Phys. Lett.* **1978**, *58*, 340.

0002-7863/91/1513-2850$02.50/0